

INCOMPRESSIBLE STATES IN DOUBLE QUANTUM DOTS.

N. Barberán and J. Soto

Departament d'Estructura i Constituents de la Matèria

Facultat de Física, Universitat de Barcelona, E-08028 Barcelona, Catalonia, Spain

Abstract

Incompressible (magic) states of vertically coupled quantum dots submitted to strong magnetic fields such that only the lowest Landau level is relevant are studied within an exact diagonalization calculation for $N = 3, 5$ and 6 , electrons. We find that the sequences of total angular momentum M for which incompressible states exists depend on the interplay between the inter-dot hopping parameter Δ_t and the inter-dot distance d . For d of the order of the magnetic length and for all values of Δ_t , we conclude that, in contrast to previous claims, the incompressible states appear at magic values of M which do not differ from those obtained for a single dot, namely $M = N(N - 1)/2 + jN$ where j is a positive integer number. For large inter-dot distance and simultaneously small inter-dot hopping parameter, new sequences of magic values of M are observed. These new sequences can be easily understood in terms of a transition regime towards a system of two decoupled single dots. However, important differences in the nature of the incompressible ground states are found with respect to those of a single dot.

KEYWORDS: Quantum Hall effect, double quantum dot, incompressible (magic) states.

PACS: 73.21-b, 73.43-f, 73.21.La, 73.43-Lp.

I. Introduction

Much effort has been devoted to understand the magic incompressible states (ISs) of electronic nanostructures. This is due to the fact that they are closely related to the states that determine properties like superconductivity or the fractional quantum Hall effect¹, which are striking examples of the non-trivial behavior that strongly interacting electronic systems may display². Finite systems like quantum dots (QD) provide simpler physical realizations of strongly interacting electronic systems where different models can be tested. When they are submitted to strong magnetic fields, the projection of the system to the lowest Landau level (LLL) becomes a good approximation which greatly simplifies theoretical studies in general, and, in particular, makes exact diagonalization calculations feasible. Much work has been done on single QD in the LLL regime yielding a reasonable understanding of the nature of their IS^{3,4}. Double quantum dots (DQD) in a vertical configuration submitted to strong magnetic fields provide another finite system in which the existence of incompressible states is expected. However, the additional degree of freedom, together with the two new parameters, namely the distance between the dots and the tunneling strength, may give rise to new phenomenology. Moreover, correlation effects can be experimentally detected in the far infrared range (FIR) using uniform electric fields with non-vanishing component along the vertical direction as the generalized Kohn theorem, under such condition does not apply⁵.

This paper is organized as follows. In Section II we describe the model used in our calculation and analyze the Hamiltonian of the system. In Section III we begin with a review of the results previously obtained for single dots and we show next our main results for double dots, which cover a wide range of input parameters. Finally, in Section IV we compare our findings with previous results in the literature and draw our conclusions.

II. The Hamiltonian

We consider two identical two-dimensional quantum dots (in a vertical configuration) confined to the XY-plane by equal parabolic potentials and submitted to a strong magnetic field directed along an arbitrary direction. The Hamiltonian of the system reads,

$$H = H_0 - H_t + H_{int} \quad (1)$$

where H_0 is the single-particle part which contains the kinetic contribution, the confining potential and the Zeeman term. We adjust the input parameters in such a way that Landau level mixing is negligible. Then, in second quantization formalism is given by

$$H_0 = \alpha M + \beta N - \Delta_Z S_B \quad (2)$$

where

$$\alpha = \frac{\hbar}{2}(\sqrt{\omega_c^2 + 4\omega_0^2} - \omega_c) , \quad (3)$$

$$\beta = \frac{\hbar}{2} \sqrt{\omega_c^2 + 4\omega_0^2} , \quad (4)$$

and

$$\Delta_Z = \mu_B g B \quad (5)$$

ω_0 being the confining potential frequency, ω_c the cyclotron frequency given by $\omega_c = eB/m^*c$ (m^* is the effective electron mass, B the magnetic field and e and c the electron charge and the speed of light in vacuum respectively), $\mu_B = e\hbar/2mc$ the Bohr magneton and g the Landé factor. $M = \sum_{i=1}^N m_i a_{\sigma_i}^+ a_{\sigma_i}$ is the total angular momentum and N is the total number of electrons. $a_{\sigma_i}^+$ creates a single particle state and σ_i refers to the three indexes that characterize the single particle wave functions: angular momentum, spin and isospin (s or a associated to symmetric and antisymmetric combinations of wave functions concentrated in each dot: right and left). The tunneling term is given by

$$H_t = \frac{\Delta_t}{2} X \quad (6)$$

where Δ_t is the energy gap between the symmetric and antisymmetric states in the noninteracting system and $X = N_S - N_A$ is given by the balance between symmetric and antisymmetric states. Finally the interacting part of the Hamiltonian is given by

$$H_{int} = \frac{1}{2} \sum_{ijkl} \sum_{\Lambda=1}^3 V_{ijkl}^{(\Lambda)} a_{\sigma_i}^+ a_{\sigma_j}^+ a_{\sigma_l} a_{\sigma_k} , \quad V_{ijkl}^{(\Lambda)} = \langle ij | V^{(\Lambda)} | kl \rangle \quad (7)$$

where the index Λ is used to distinguish between the three different possibilities: (i) $V^{(1)} = 0$ when only one change of a single particle isospin takes place, (ii) $V^{(2)} = \frac{1}{2}(V_{rr} + V_{rl})$ when both isospins remain unchanged and (iii) $V^{(3)} = \frac{1}{2}(V_{rr} - V_{rl})$ when both isospins are changed⁵. V_{rr} and V_{rl} are the intra and inter-dot Coulomb potentials respectively, which are given by

$$V_{rr} = \frac{e^2}{\epsilon r} \quad (8)$$

and

$$V_{rl} = \frac{e^2}{\epsilon(r^2 + d^2)^{1/2}} , \quad (9)$$

d being the distance between the dots along the z -direction, \vec{r} a 2-dimensional vector and ϵ is the dielectric constant of the host semiconductor. We have assumed Dirac-delta distributions along the z -direction and have taken as a basis, Slater determinants built up from Foch-Darwin single particle wave functions projected on the LLL³. The diagonalization can be performed in separated subspaces characterized by three well defined quantum numbers: the total angular momentum M , the total spin S along the direction of the field \vec{B} and the parity P related to the reflexion symmetry on the z -direction (P defined as $P = (-1)^{X/2}$ for even N and $P = (-1)^{(X+1)/2}$ for odd N). We will define the set (M, S, P) as a configuration.

The eigenstates within each configuration are determined by $H_{int} - H_t$ alone, and the role of the constant term given by H_0 is to shift the eigenenergies as a whole without changing their relative order.

III. Incompressible states

Before studying the incompressible states in DQDs, we briefly review previous work on single quantum dots and its consequences. For a QD an IS with total energy E and characterized by (M, S, P) is identified as the one which has the following singular property: the lowest excited state with quantum numbers $(M + 1, S, P)$ has energy $E + \alpha$. That is to say, the energetically most favorable way to excite an IS increasing its total angular momentum by one unit is by moving the system as a whole, namely by increasing by one unit the angular momentum of the center of mass only and leaving the internal structure unchanged, i.e., without producing an expansion that would decrease its internal energy. This characteristic was nicely recognized analyzing the Coulomb contribution to the total energy as a function of M . A periodical arrangement of plateaux (steplike structure) in the otherwise decreasing curve signaled the values of the magic angular momenta⁶. Furthermore, the variation of the magnetic field (or the confining potential) did not drive the ground state through all neighboring values of M but through the sequence of magic values only⁷.

This scenario corresponds to the regime characterized by a filling factor lower or equal to one, defined as⁶

$$\nu = \frac{N(N - 1)}{2M} \quad (10)$$

which involves the minimum possible value of the total angular momentum for a full polarized QD given by $M_{min} = N(N - 1)/2$ (the "compact state") and the angular momentum M of the magic state. The filling factor refers to the number of sublevels occupied within the LLL. There are two sublevels (spin up and down) in the case of a single QD and four (two for spin and two for isospin) in the case of a DQD. In general, for regimes in which several sublevels are occupied, the filling factor of a QD is not well defined. Ground states which are not related with incompressible states are also possible under such multiple-sublevel occupancy.

The sequence of magic filling factors depend on the number of electrons, for $N = 3$ the values of ν are $\nu = 1, \frac{1}{2}, \frac{1}{3}, \frac{1}{4}, \dots$ or for $N = 4$ they are $\nu = 1, \frac{3}{5}, \frac{3}{7}, \frac{1}{3}, \dots$, in both cases related to the magic angular momentum given by

$$M = \frac{1}{2}N(N - 1) + jN \quad (11)$$

where j is a positive integer number. It turns out that the analysis of the Coulomb contribution to the total energy as a function of M gives exhaustive and precise information about the magic values of the angular momentum and hence about the magic filling factors. The magic values of M are the initial values of the plateaux. However, no information about the total spin of the ISs comes from the previous analysis. In the $N = 3$ case, for a QD, the sequence of ground states is always full polarized ($S_z = 3/2$) if the Zeeman term is included in the Hamiltonian (with $|g| = 0.44$) or in contrast, oscillations between $S_z = 3/2$ and $S_z = 1/2$ were obtained if no Zeeman term is included in the calculation^{6,7}. However, in the last case, the wild changes in spin and angular momentum do not appear simultaneously.

If the evolution of the ground state of a single QD from $\nu = 1$ as B grows up is studied, the first ground state obtained is the compact state. The compact state belongs to a one dimensional subspace and, as a consequence, no correlation is involved as one Slater determinant produces the exact solution. Moreover, the density is a "dome" shape circular symmetric distribution without any structure. As B grows, the angular momentum jumps from M to $M + N$, all the electrons jump together moving away from the origin and forming a ring. The dimension of the ground state subspace increases and as the relative weights of the different Slater determinants within the expansion of the ground state function become significant for several different elements of the bases, namely the correlation becomes important.

Some care must be taken for low values of B for which the assumption of the LLL regime is not fulfilled. A suitable way to check this condition is given by the value of n , defined as the integer part of ω_+/ω_- (where $\omega_{\pm} = \frac{1}{2}(\sqrt{\omega_c^2 + 4\omega_0^2} \pm \omega_c)$), which is related to the number of different single-particle states that fit into the LLL below the energy of the second Landau level.

For a DQD we have a richer parameter space to be explored as, in addition to the parameters of a single QD, Δ_t and d also enter the Hamiltonian, which open new possibilities for ISs to exist. We will focus on the phase diagram (Δ_t / d) for standard values of the remaining input parameters. Due to the fact that Coulomb interaction and changes in parity are coupled processes in a DQD, we define the internal energy as the Coulomb plus the tunneling contribution.

For $d \sim l_B$ the pure Coulomb contribution to the total energy ($\alpha = \beta = \Delta_t = \Delta_Z = 0$) as a function of M , is a decreasing function without plateaux as it is shown in the curves (a) in Fig.1 (for $N = 5$) and 2 (for $N = 6$) (energies are given in units of $u = e^2/\epsilon l_B$, $l_B = \sqrt{\frac{\hbar}{m(\omega_c^2 + 4\omega_0^2)^{1/2}}}$). Figs.1A and 2A correspond to parity $P = 1$ and Figs.1B and 2B to $P = -1$. All four cases refer to full polarized systems ($S=5/2$ for $N=5$ and $S=3$ for $N=6$) . For each value of M , the energy displayed is the lowest within the configuration (M, S, P) . The absence of plateaux can be understood as follows. Since $\Delta_t = 0$, the number of electrons in each dot is a well defined number. Hence, in order to increase the total angular momentum by one unit, the angular momentum of either dot must be increased by one unit, which unavoidably increases the typical distance from the electrons of one dot to the ones of the other dot, and, therefore, decreases the inter-dot Coulomb energy.

According to Figs.1 and 2 ($d \sim l_B$), it is necessary to include a sizeable tunneling contribution in order to obtain a sequence of plateaux, which, furthermore, only occur for $P = -1$. Indeed, from a series of calculations for $N = 5$ (not shown in Figs.1), which correspond to a variation of Δ_t from 0 to 2 meV, we see a number of plateaux gradually appearing as Δ_t increases. We find that from $\Delta_t = 2$ meV to 0.8 meV the section from $M = 10$ to $M = 11$ and from $M = 15$ to $M = 16$ are exact plateaux. For $\Delta_t = 0.4$ meV they are approximately plane and for $\Delta_t = 0.2$ meV they disappear. However in all cases the curves are abruptly decreasing before $M = 10$ and between magic values. That is to say, we do not find any extra value of magic M different from those given by Eq.(11).

In order to obtain information about the spin and parity of the incompressible states, we calculated the Coulomb plus tunneling contribution for all possible configurations. Fig.3 (for $N = 5$) shows that the sequence of plateaux appear only when the system is fully polarized in spin and have parity $P = -1$ (similar results were obtained for $N = 6$). Furthermore, although the parity $P = -1$ for $N=5$ can be obtained from different values of X , i.e., $X = N_S - N_A = 5, 1$ or -3 , the occupancy of the single-particle states for such incompressible ground states turns out to be $X = 5$ only, namely the system is always full spin and isospin polarized. This suggests that the incompressible state will not present variations in S as B increases. This last suggestion was confirmed, for Zeeman contribution different from zero in the Fig.4 where the total energy of the ground state as a function of the magnetic field is shown. The arrows point to the places where the angular momentum jumps from one magic value to the next one, leaving the spin and parity unchanged. In the inset we show $E_{GS} - \beta N$ in order to compare with other publications which omit the N -dependent term. The nearly monotonous function of B is due to the fact that, in the absence of spin or isospin transitions, the internal energy has a negligible influence in the plot and hence the evolution of the system is driven by the monotonous increasing term βN which is much more important than the decreasing term αM , which would produce kinks at the transition points, as it is shown in the inset ($E_{gs} - \beta N$ versus B).

The single particle occupancies of the m -values for the first three ISs for $N = 5$, calculated at $B = 4, 7$ and 9 T respectively are shown in Fig.5. As it was discussed before and apparent from this figure, the electrons form a ring which moves away from the origin and slightly enlarges its width as M increases.

If the Zeeman term is omitted, it comes out that the three possible spin configurations, i.e., $S = 5/2, 3/2$ and $1/2$ are degenerated at the magic values of M , as it appears in Fig.3A. Incidentally, this degeneracy may allow the presence of spin textures. This turns out to be an important difference from a single QD. As it was discussed previously, for a QD without Zeeman interaction, the incompressible ground state changes its spin as B increases⁷ in contrast with our findings for a DQD.

It should be noted that the reproduction of Eq.(11) for a DQD could be beforehand predicted due to the fact that a single QD full spin polarized and a DQD both full spin and isospin polarized are equivalent systems with no extra degree of freedom besides the angular momentum.

So far we have explored the situation $d \sim l_B$. In order to get the complete scenario of ISs in a DQD, we have also investigated in detail the remaining regions of the phase diagram (Δ_t / d)

In Figs.6-9 we follow, for $N=3$, the variation of the internal energy as d and Δ_t change. From A to B (Fig.6), as it was just discussed for $d \sim l_B$, the plateaux emerge as Δ_t grows from zero until they are well defined at $\Delta_t = 0.11$ u . From B to C (Fig.7), although the distance d grows, the sequence of plateaux does not change as tunneling is always allowed. From A to D (Fig.8), (where tunneling is small) starting from a curve without plateaux of a DQD, we move across a transition regime with a gradual formation of new plateaux at $M = M_1 + M_2$ where M_1 and M_2 are magic numbers of a single QD.

We come close to the point D which corresponds to two decoupled dots with $N = 1$ and $N = 2$ respectively. Finally from D to C (Fig.9), the tunneling gap increases and the system of two decoupled QD with a period of two typical of the $N = 2$ single dot ($N = 1$ has no Coulomb energy) evolves into a DQD reproducing a period of three typical of the $N = 3$ DQD. This interesting transition had not been observed before.

For d close to zero and Δ_t large (at the left of point B), the internal energy of a single QD can be reproduced with high accuracy by the subtraction of the constant contribution $\Delta_t X$ to the energy. This fact allowed us to study the evolution of the $N=5$ DQD which turned out to be more intricate. Nevertheless, it can also be fully explained in a similar way, that is to say, as the combined manifestation of a DQD and two decoupled $N = 3$ and $N = 2$ dots at D.

IV. Discussion

We have investigated in detail the existence of ISs in a DQD for the entire phase diagram (Δ_t / d).

An important point in our analysis is the criterium used to identify ISs. As discussed in the previous section, we define the internal energy as the Coulomb plus tunneling contributions, and require IS to preserve the internal energy when the angular momentum M is increased by one unit. We want to stress that this is not equivalent to identifying magic M from the kinks of the lowest energies of each configuration as a function of M or from the kinks of the variation of the absolute ground state energy as a function of B , as it has been used in the literature^{8,9}.

For $d \sim l_B$ the fact that the magic M follow Eq.(11) is in conflict with the claim made in Ref.^{8,9} that extra magic values for M (depending on the value on the tunneling strength) exist in this regime. The authors of Ref.^{8,9} identified ISs with downward cusps of the total energy as a function of M , i.e. the internal energy (our curve) with the addition of the single-particle contribution. In Fig.10 we show the two possibilities for $N = 5$. It is clear from the upper curve that some downward cusps, which would be identified as ISs by the criterium of Ref.^{8,9}, do not actually correspond to ISs. We claim that, the right criterium in order to find the magic values of M is by the analysis of the internal energy contribution (Coulomb plus tunneling for DQD) and not by the analysis of the structure of the total energy.

In order to make sure that the discrepancies with Ref.^{8,9} are only due to the different criteria to identify ISs, we have reproduced their results (see Fig.11). To be more precise, we performed the calculation for $N = 3$ and the same input parameters as those used in Ref.⁸ ($N = 3$, $B = 15 T$, $d = 200 \text{ \AA}$, $\hbar\omega_0 = 3 \text{ meV}$ and $\Delta_t = 0.2 \text{ meV}$). In Fig.11A the internal energy contribution versus M is shown. Due to the low value of the tunneling contribution, the plateaux that will appear, for larger values of Δ_t , at $M = 3, 6$ and 9 are still not visible and the only ones that already appear are $M = 12$ and 15 . If the kinetic contribution is added, it comes out that the ground state is at $M = 5$ (see Fig.11B) at the lowest downward cusp of the total energy in accordance with Ref.⁸. It is unquestionably the ground state, however it is not an incompressible magic state.

Our conclusions can be summarized as follows:

- (i) The unambiguous criterium to identify the IS is by the analysis of the plateaux that appear in the curve of the internal energy versus M .
- (ii) For $d \sim l_B$, it is not possible to obtain ISs if the tunneling is small.
- (iii) For $d \sim l_B$ and no Zeeman term, all spin configurations are degenerate within the ground state, but only the full polarized one is an IS.
- (iv) For $d \sim l_B$ and arbitrary Δ_t or for large Δ_t and arbitrary d , the ISs are full spin and isospin polarized ($S = N/2$, $X = N$) whenever they are the ground state of the system (even if $\Delta_Z = 0$). The magic values M obey Eq. (11).
- (v) For small Δ_t , as d grows, the DQD evolves into two decoupled single QDs. New magic values M appear which correspond to the addition of magic numbers of two decoupled QDs.
- (vi) The ISs are the only possible ground states for ν lower than one. However without this constriction, other ground states are possible.

Before closing, let us briefly elaborate on the last point. Notice that the following situations are also possible: (a) ground states with M that fulfills Eq. (11) and are not ISs due to the fact that from M to $M + 1$ there is not a plateau. This condition can be obtained for very low values of Δ_t , for example, for $N = 5$, $M = 10$, $B = 5T$, $\hbar\omega_0 = 2.6\text{ meV}$, $\Delta_t = 0.2\text{ meV}$ and $d = 20\text{ \AA}$. The system is nearly full isospin polarized, however the Coulomb plus tunneling ($E(C+T)$) contribution is not constant from M to $M + 1$. (b) Ground states with M not given by Eq. (11) for which the system is not full spin or isospin polarized, (or $\nu > 1$) and $E(C+T)$ has not a constant evolution from M to $M + 1$. This is the case for example for $N = 5$, $M = 13$ ($B = 6T$, $\hbar\omega_0 = 2.6\text{ meV}$ $d = 20\text{ \AA}$ and $\Delta_t = 5.86 \cdot 10^{-3}\text{ meV}$). In the last case, $S = N\sigma$ (σ being the single-particle spin) and $P = -1$, however $X \neq N$.

Notice also that the previously discussed states are not the only possible ground states within the LLL regime. For instance, if the confining potential is strong enough, other types of ground states are possible like the ferromagnetic, canted and symmetric states (all of them with $\nu = 2$) first studied in double layers¹⁰ and latter recognized in DQD¹¹.

Finally, let us note that the correlation plays an increasingly important role as the magnetic field grows up. The system evolves from the first possible IS, namely the "compact state" where correlation is absent, to states of increasing complexity for which the expansion in Slater determinants include a larger number of elements with significant weight. The internal energy and correlation effects can be experimentally tested by uniform electric fields with non-vanishing component along the z-direction due to the fact that under this condition, the Kohn theorem does not apply⁵ and the FIR spectroscopy becomes sensitive to the internal structure.

We gratefully acknowledge C. Tejedor and L. Martín-Moreno for the code used for the Hamiltonian diagonalization. This work has been performed under Grants No. BFM2002-01868 from DGESIC (Spain), No. FPA2001-3598 from MCyT and Feder (Spain), and No. 2001GR-0064 and No. 2001SGR-00065 from Generalitat de Catalunya.

REFERENCES

- ¹ R.B. Laughlin, Phys. Rev. **B27**, 3383 (1983).
- ² R.E. Prange, S.M. Girvin, Editors, "The Quantum Hall Effect" (Springer-Verlag, New York, 1990).
- ³ L. Jacak, P. Hawrylak and A. Wjs, "Quantum Dots" (Springer Verlag, Berlin, 1998).
- ⁴ T. Chakraborty, "Quantum Dots" (North-Holland, Amsterdam, 1999).
- ⁵ N. Barberan, J. Soto, cond-mat/0204561, to appear in Phys. Rev. B.
- ⁶ P.A. Maksym and T. Chakraborty, Phys. Rev. Lett **65**, 108 (1990).
- ⁷ P. Hawrylak, D. Pfannkuche, Phys. Rev. Lett **70**, 485 (1993).
- ⁸ H. Imamura, P.A. Maksym and H. Aoki, Phys. Rev. **B53**, 12613 (1996).
- ⁹ H. Imamura, P.A. Maksym and H. Aoki, Phys. Rev. **B59**, 5817 (1999).
- ¹⁰ S. Das Sarma, S. Sachdev and L. Zheng, Phys. Rev. **B58**, 4672 (1998).
- ¹¹ L. Martin-Moreno, L. Brey and C. Tejedor, Phys. Rev. **B62**, R10633 (2000).

FIGURES

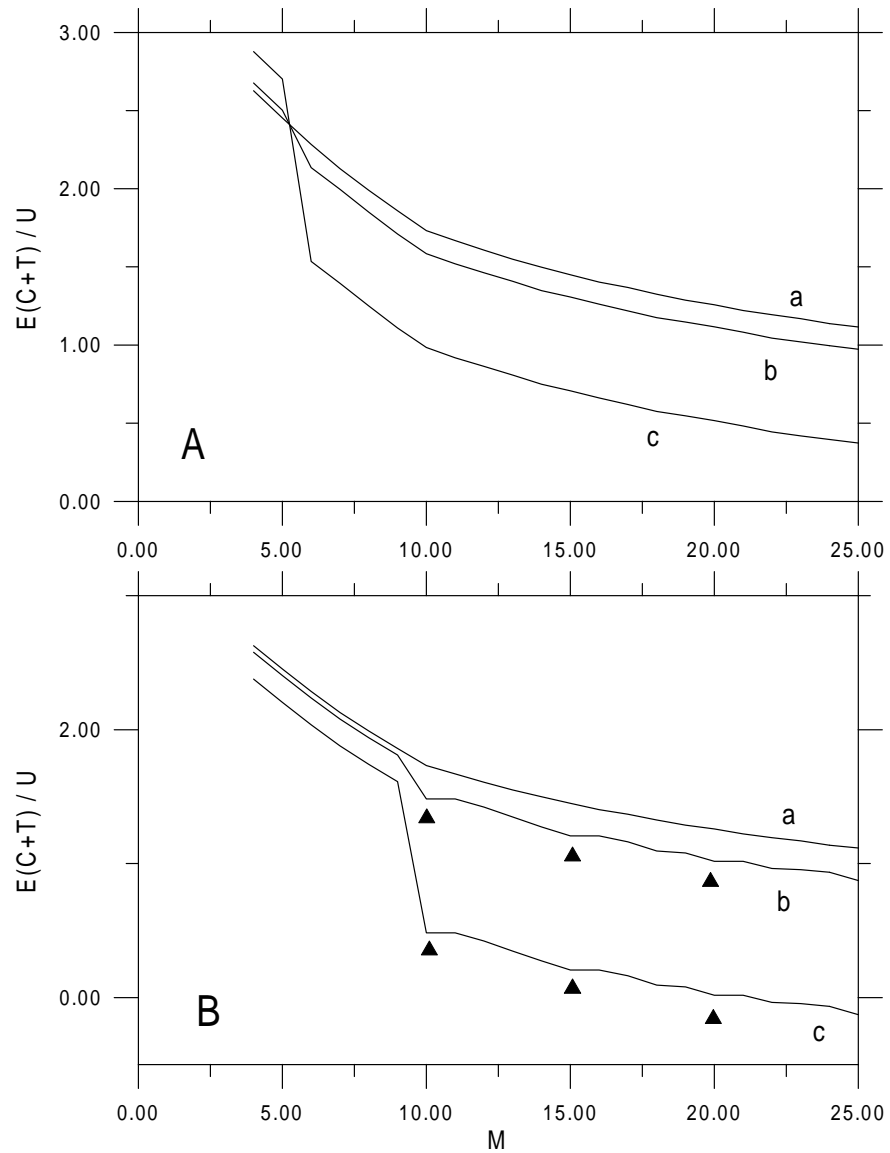


FIG. 1. A: Coulomb plus tunneling contribution to the total energy as a function of M for $N = 5$, $S = N/2$ and parity $P = 1$, for several values of the tunneling gap: (a) $\Delta_t = 0$, (b) $\Delta_t = 2.2 \text{ meV}$ and c) $\Delta_t = 11 \text{ meV}$. B: The same as A for $P = -1$. The triangles point to the beginning of the plateaux. We have taken $B = 5T$, $d = 20\text{\AA}$, and $\hbar\omega_0 = 2.6 \text{ meV}$.

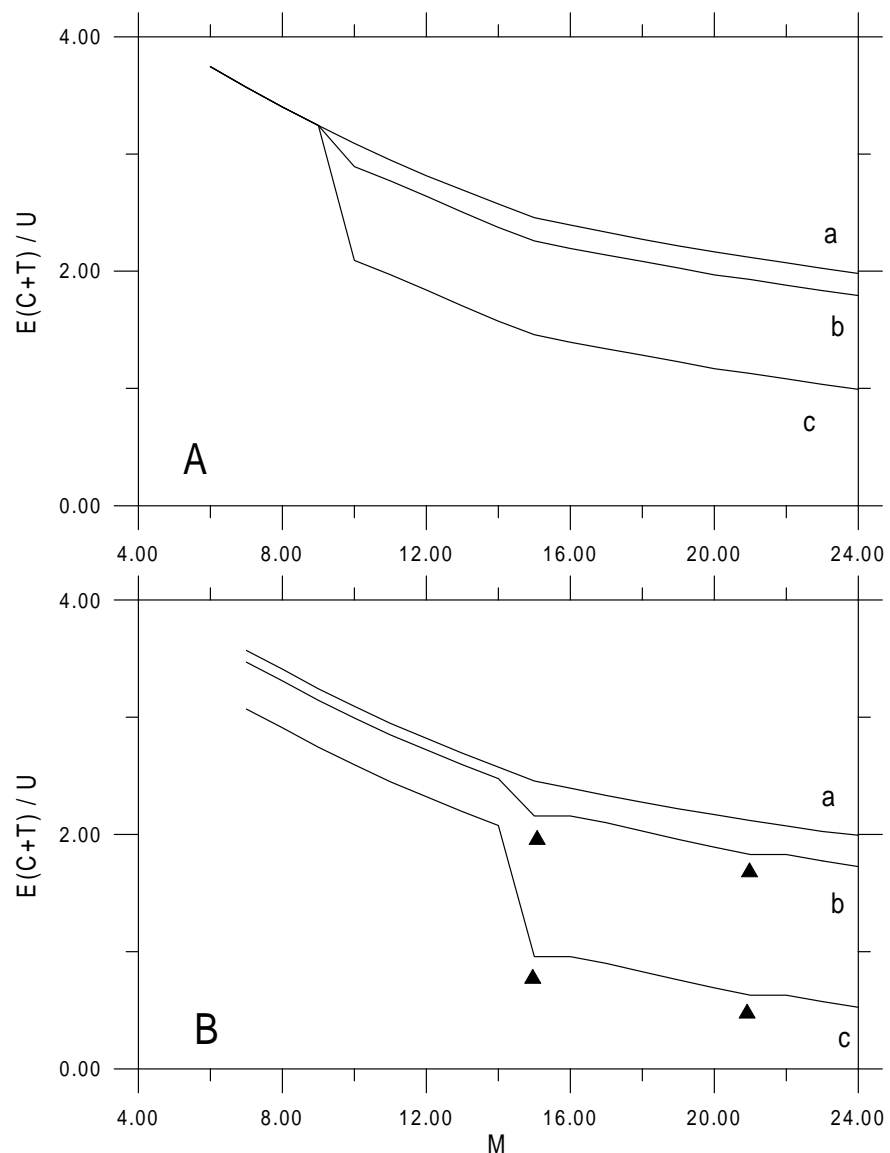


FIG. 2. The same as Fig.1 for $N = 6$

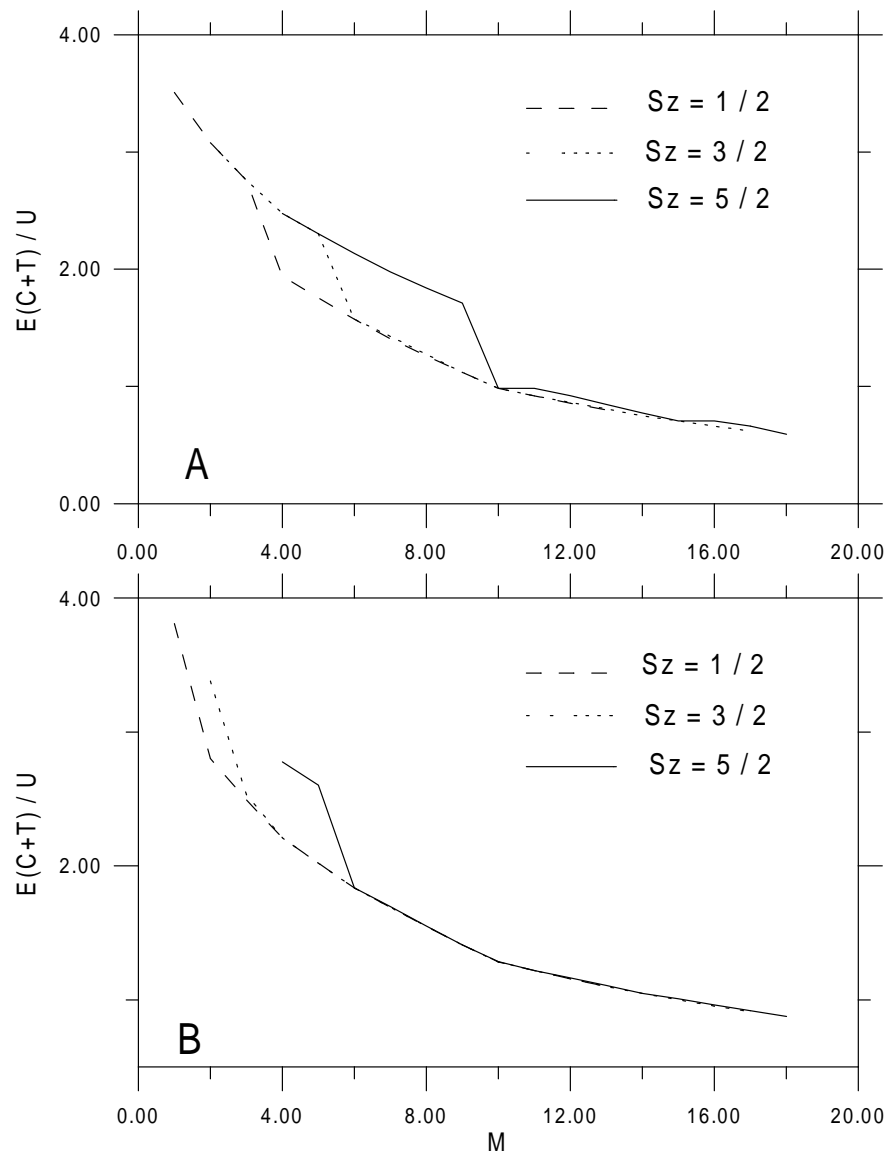


FIG. 3. A: Coulomb plus tunneling contribution to the total energy as a function of M for $N = 5$ and parity $P = -1$ for all the possible values of the spin S . B: The same as A for $P = 1$. We have taken $B = 5T$, $d = 20\text{\AA}$, $\hbar\omega_0 = 2.6\text{ meV}$ and $\Delta_t = 2\text{ meV}$.

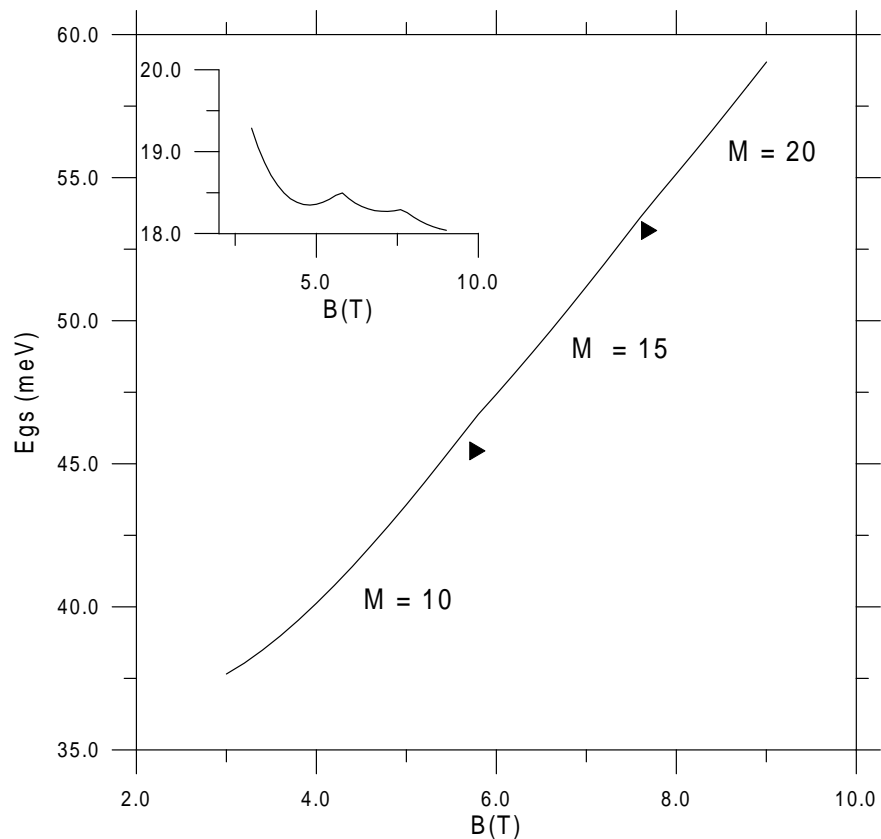


FIG. 4. A: Ground state energy versus B for $N = 5$. The triangles point to the transitions between magic angular momenta. We use the same values for d , ω_0 and Δ_t as in Fig.3. Inset: $E_{gs} - \beta N$ as a function of B .

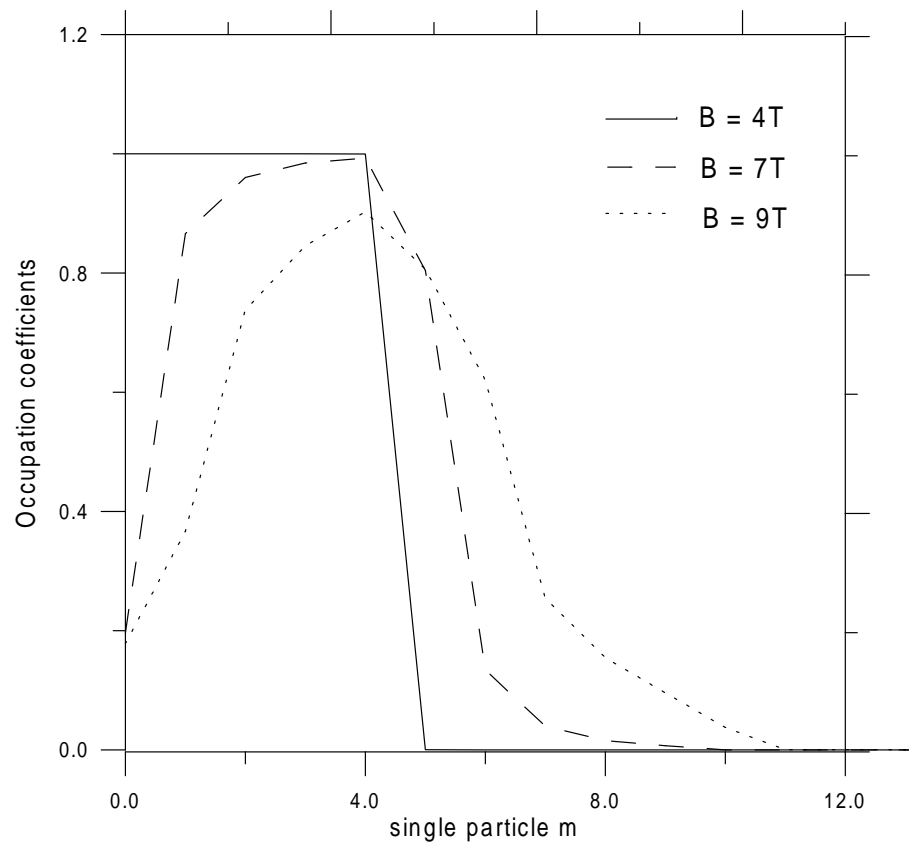


FIG. 5. Total occupancy of the single-particle angular momentum states m for $N = 5$. The values of B considered correspond to the magic values $M = 10, 15$ and 20 respectively. We have taken $d = 20\text{\AA}$, $\hbar\omega_0 = 2.6\text{ meV}$ and $\Delta_t = 6\text{ meV}$.

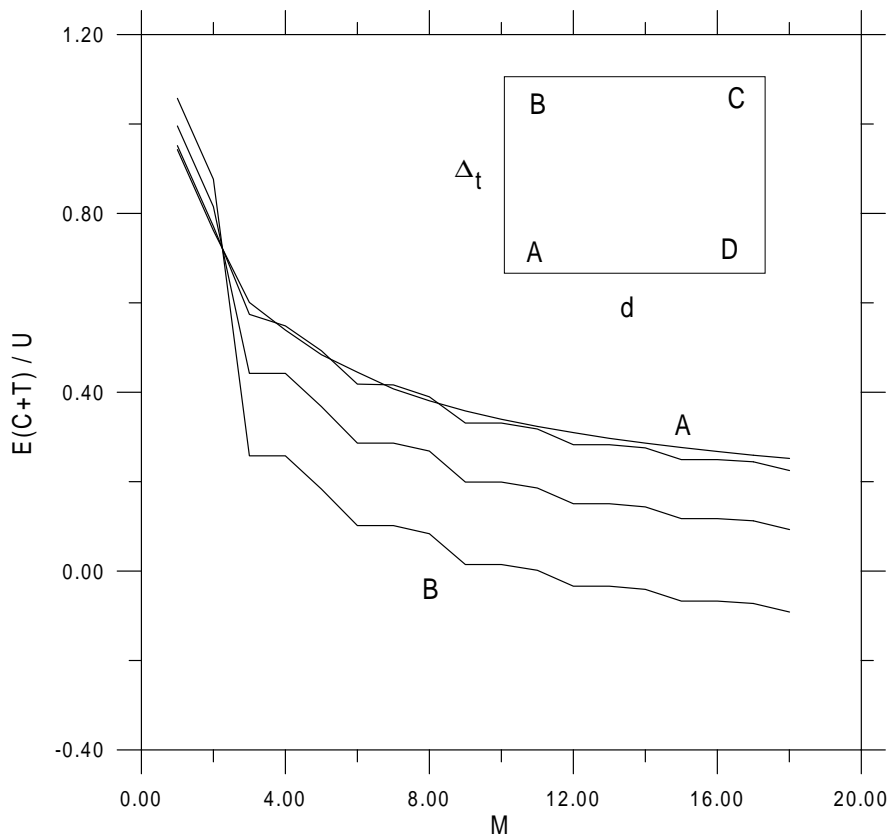


FIG. 6. Coulomb plus tunneling contribution versus M for $N = 3$. From A to B the tunneling gap is: 0.0, 0.018, 0.106 and $0.229u$ respectively. Inset: phase diagram used. We have taken $\hbar\omega_0 = 2.6\text{ meV}$, $B = 15\text{T}$, $d = 10\text{\AA}$, $S = 3/2$ and $P = -1$.

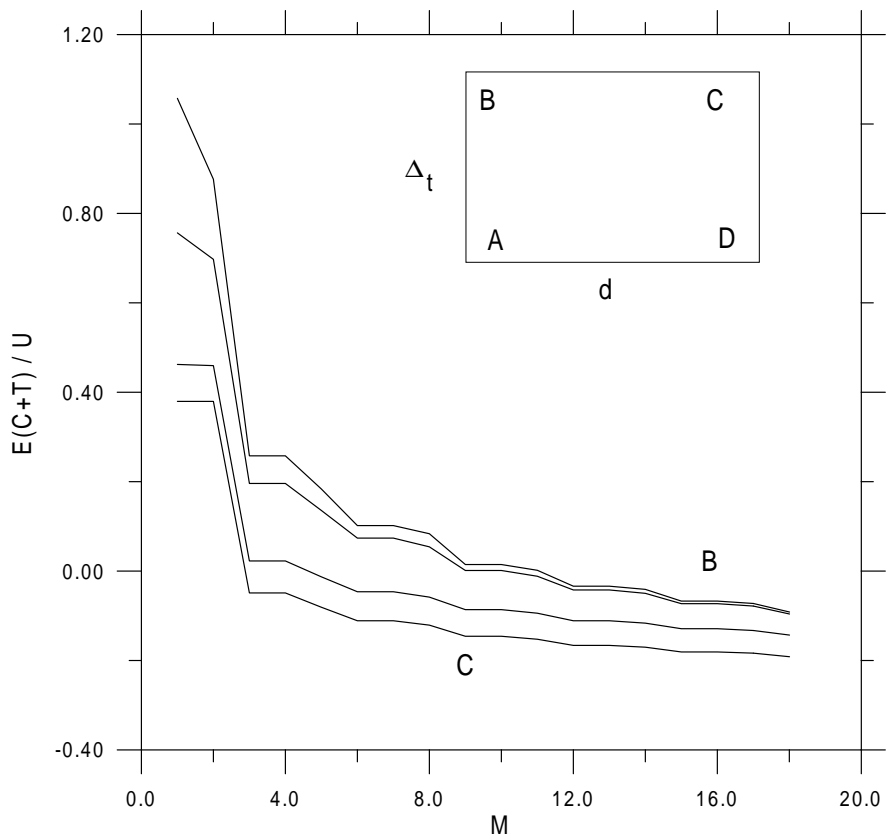


FIG. 7. The same as Fig.6 for $\Delta_t = 0.229$ u . From B to C the inter-dot distance is: 50, 100, 500 and 1000 \AA respectively. Inset: phase diagram used.

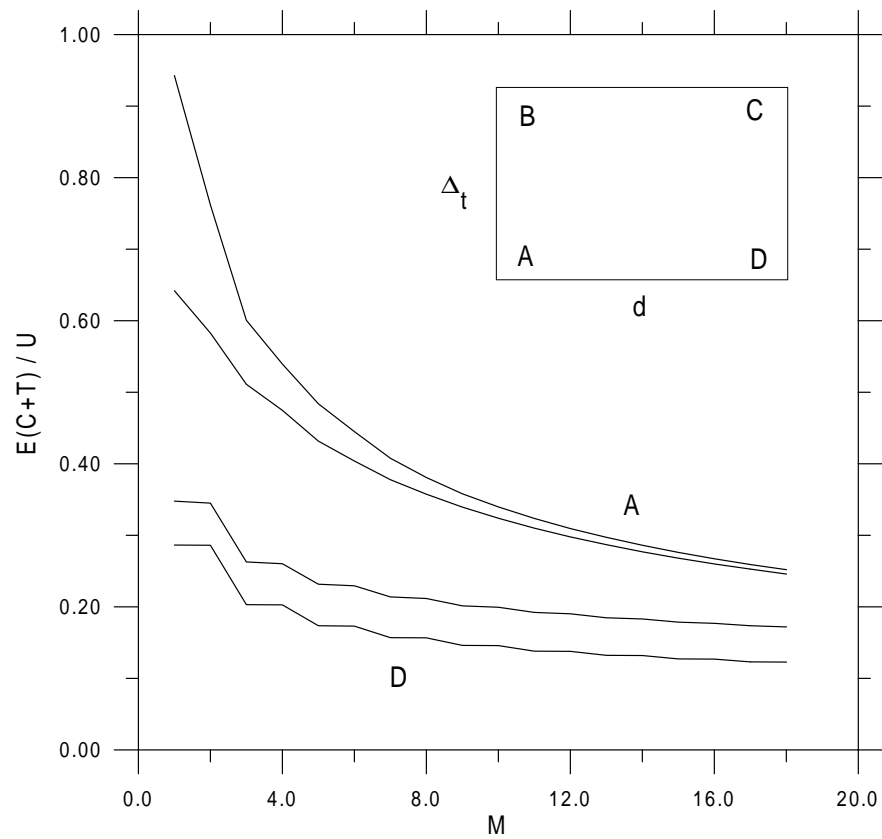


FIG. 8. The same as Fig.6 for $\Delta_t = 0$. From A to D the inter-dot distance is: 10, 50, 500 and 1000 \AA respectively. Inset: phase diagram used.

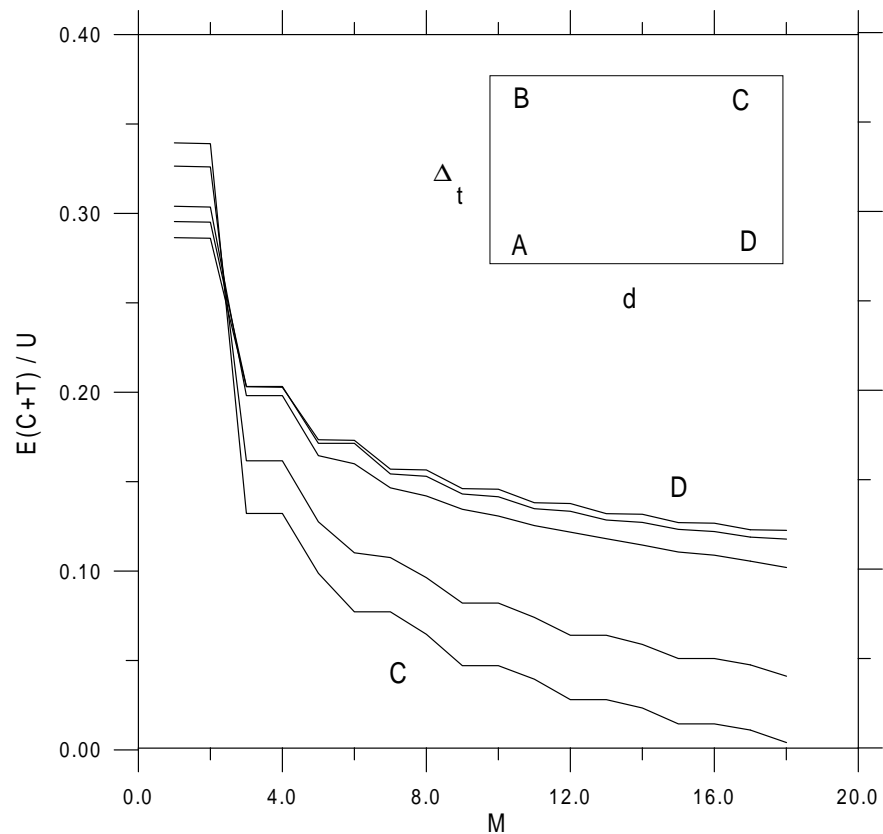


FIG. 9. The same as Fig.6 for $d = 1000 \text{ \AA}$. From D to C the tunneling gap is: 0.0, 0.018, 0.035, 0.080 and 0.106 u respectively. Inset: phase diagram used.

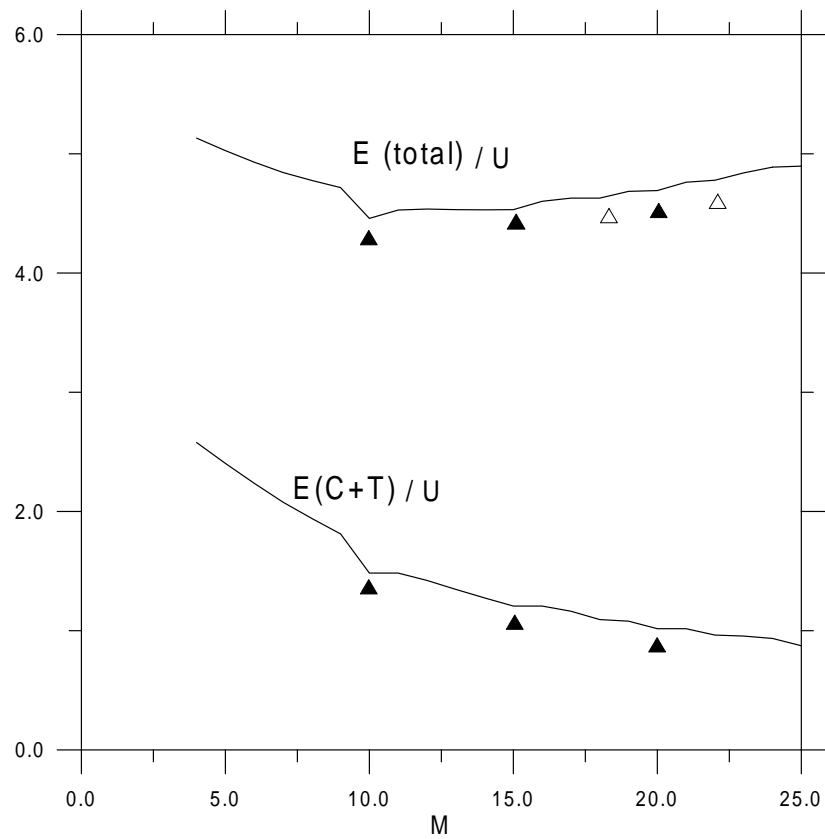


FIG. 10. Coulomb plus tunneling contribution (lower curve) and total energy (upper curve) as a function of M for $N = 5$. The black triangles point to the actual magic values M whereas the white triangles point to cusps which could be mistaken by them. The values of B , ω_0 , d and Δ_t are the same as in Fig.3

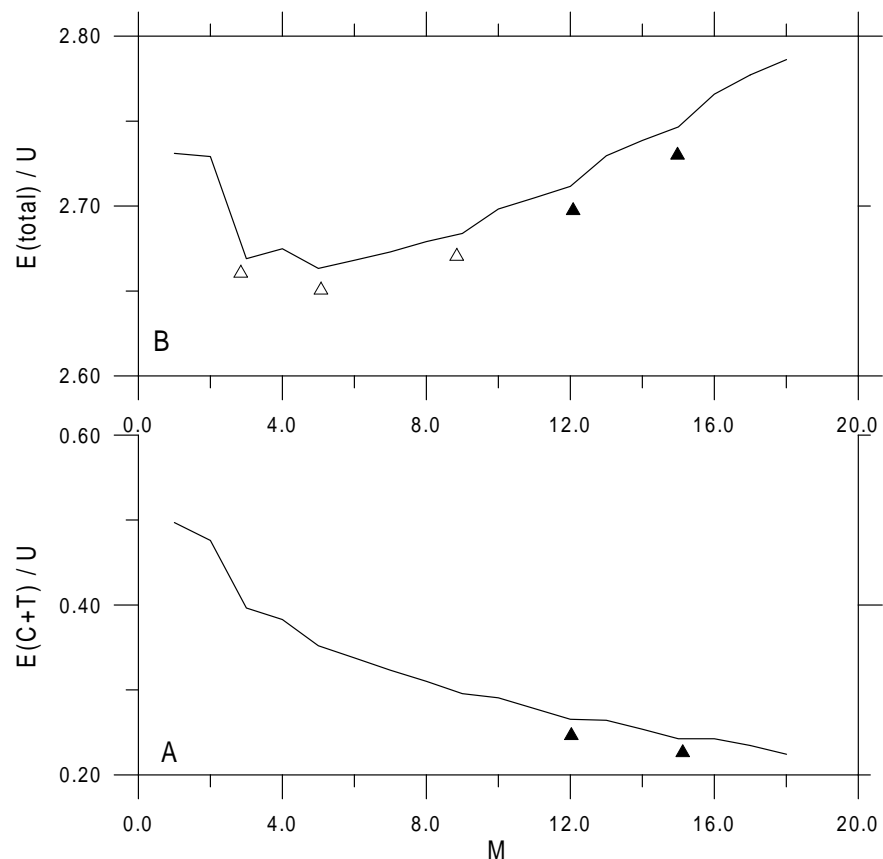


FIG. 11. A: Coulomb plus tunneling contribution versus M for $N = 3$. B: The same as in A for the total energy. The input parameters are given in the text. The black triangles point to the actual magic values M whereas the white triangles point to cusps which could be mistaken by them.